J|A|C|S
ARTICLES
Published on Web 03/25/2004

Dirhodium Tetracarboxylate Scaffolds as Reversible Fluorescence-Based Nitric Oxide Sensors

Scott A. Hilderbrand, Mi Hee Lim, and Stephen J. Lippard*

Contribution from the Department of Chemistry, Massachusetts Institute of Technology, Cambridge, Massachusetts 02139

Received September 11, 2003; E-mail: lippard@lippard.mit.edu

Abstract: We report the synthesis and characterization of dirhodium tetracarboxylate complexes $[Rh_2(\mu\text{-}O_2CR)_4(L)_2]$, with R = Me and L = dansyl-imidazole (Ds-im) or dansyl-piperazine (Ds-pip). The fluorophores coordinate to the axial sites of the dirhodium core through the imidazole or piperazine N-atom and emit only weakly when excited at 365 or 345 nm for the Ds-im and Ds-pip complexes, respectively. These fluorophore-containing complexes were investigated for their ability to elicit a fluorescence response in the presence of NO. An immediate increase in fluorescence emission of greater than 15-fold occurs when NO is admitted to solutions containing $[Rh_2(\mu\text{-}O_2CMe)_4]$ and Ds-pip or Ds-im. In both systems, the fluorescence response, which arises by NO-induced displacement of the axially coordinated fluorophore, is reversible with a sensitivity of $\sim$4 μM. The related dinitrosyl complexes $[Rh_2(\mu\text{-}O_2CR)_4(NO)_2]$, where R = Me, Et, or *n*-Pr, were prepared, structurally characterized, and found to be air-stable, losing NO upon standing in solution. Sequestration of a methylene chloride solution of the Ds-pip complex from aqueous media by a NO-permeable membrane allows for fluorescence detection of NO for potential applications in biological fluids.

Introduction

Nitric oxide (NO), a neutral inorganic molecule with one unpaired electron, has received considerable attention since its identification as a signaling agent in biological systems.[1] Recent research implicates involvement of NO in physiological processes such as vasodilation,[2] carcinogenesis,[3,4] neurodegenerative disorders,[5] and neurotransmission.[6] Current work focuses on the use of NO donor compounds and nitric oxide synthase inhibitors to elucidate additional biological functions.[7,8] A sensor capable of direct, reversible detection of NO would be invaluable to advance our understanding of its roles in biology.

NO detection methodologies[9] include electrochemical,[10] EPR,[11] chemiluminescent,[12] and fluorescence-based techniques.[13,14] Of these options, those based on fluorescence signaling have great potential for investigating how NO facilitates neurotransmission, an area of focus in our laboratory. Current fluorescence-based NO sensors, however, are not ideal, requiring either dioxygen[15] or an external reductant[16] to form a fluorescent species. Fiber-optic NO biosensors containing a fluorescent dye-labeled heme domain of cytochrome *c*′ or soluble guanylate cyclase (sGC) have been fabricated.[17−19] These fiber-optic detectors are based on attenuation of fluorescence emission in response to NO, instead of the more desirable analyte-induced increase in emission. Recently, we described an approach that utilizes transition-metal nitrosyl-forming reactions to monitor NO directly by ejection of a fluorescent ligand that had been quenched by coordination.[13] Related sensors using *N*-oxide-fluorophore conjugates have been described, but display a decrease in fluorescence after reaction with NO, react slowly with NO, or are air-sensitive.[14] None of the current small-molecule-based NO sensors is reversible, and thus none is capable of providing temporal data about fluctuating NO concentrations.

Our interest in developing sensors that utilize the formation of transition-metal nitrosyl complexes to trigger an increase in fluorescence is based on a strategy that takes advantage of the well-known fluorescence-quenching properties of transition metals with partially filled d-shells.[13,20,21] In particular, we have been exploring systems in which reaction of NO with a

(1) Furchgott, R. F. *Angew. Chem., Int. Ed.* **1999**, *38*, 1870−1880.
(2) Ignarro, L. J. *Angew. Chem., Int. Ed.* **1999**, *38*, 1882−1892.
(3) Lala, P. K. *Cancer Metastasis Rev.* **1998**, *17*, 1−6.
(4) Wink, D. A.; Vodovotz, Y.; Laval, J.; Laval, F.; Dewhirst, M. W.; Mitchell, J. B. *Carcinogenesis* **1998**, *19*, 711−721.
(5) Calabrese, V.; Bates, T. E.; Stella, A. M. G. *Neurochem. Res.* **2000**, *25*, 1315−1341.
(6) Prast, H.; Philippu, A. *Prog. Neurobiol.* **2001**, *64*, 51−68.
(7) Hölscher, C. *Eur. J. Pharmacol.* **2002**, *457*, 99−106.
(8) Grassi, S.; Pettorossi, V. E. *Neuroscience* **2000**, *101*, 157−164.
(9) Nagano, T.; Yoshimura, T. *Chem. Rev.* **2002**, *102*, 1235−1270.
(10) Bedioui, F.; Villeneuve, N. *Electroanalysis* **2003**, *15*, 5−18.
(11) Fujii, S.; Yoshimura, T. *Coord. Chem. Rev.* **2000**, *198*, 89−99.
(12) Brien, J. F.; McLaughlin, B. E.; Nakatsu, K.; Marks, G. S. *Methods Enzymol.* **1996**, *268*, 83−92.
(13) Franz, K. J.; Singh, N.; Lippard, S. J. *Angew. Chem., Int. Ed.* **2000**, *39*, 2120−2122.
(14) Katayama, Y.; Soh, N.; Maeda, M. *Bull. Chem. Soc. Jpn.* **2002**, *75*, 1681−1691.
(15) Kojima, H.; Nakatsubo, N.; Kikuchi, K.; Kawahara, S.; Kirno, Y.; Nagoshi, H.; Hirata, Y.; Nagano, T. *Anal. Chem.* **1998**, *70*, 2446−2453.
(16) Meineke, P.; Rauen, U.; de Groot, H.; Korth, H.-G.; Sustmann, R. *Chem.-Eur. J.* **1999**, *5*, 1738−1747.
(17) Barker, S. L. R.; Zhao, Y.; Marletta, M. A.; Kopelman, R. *Anal. Chem.* **1999**, *71*, 2071−2075.
(18) Barker, S. L. R.; Kopelman, R.; Meyer, T. E.; Cusanovich, M. A. *Anal. Chem.* **1998**, *70*, 971−976.
(19) Barker, S. L. R.; Clark, H. A.; Swallen, S. F.; Kopelman, R.; Tsang, A. W.; Swanson, J. A. *Anal. Chem.* **1999**, *71*, 1767−1772.

10.1021/ja038471j CCC: $27.50

transition-metal complex containing a coordinated fluorophore conjugate results in removal of the fluorophore from the coordination sphere of the metal with concomitant fluorescence turn-on. In the present paper, we describe the reversible fluorescence-based detection of NO with the use of dirhodium tetracarboxylate scaffolds containing bound fluorophore conjugates.

Dirhodium tetracarboxylates are air-stable compounds that coordinate a variety of ligands at the axial positions of the tetra-bridged dimetallic core.[22] The reaction of NO with solid [$Rh_2(\mu$-$O_2CMe)_4$], first reported in 1963, affords a nitrosyl adduct that can be reversed upon heating to 120 °C, although the products were not fully characterized.[23] The only crystallographically defined dirhodium nitrosyl complex is [$Rh_2(\mu$-$O_2CMe)_4(NO)$-(NO_2)], which was prepared by the reaction of [$Rh_2(\mu$-$O_2CMe)_4$] with excess NO in CH_2Cl_2.[24] We find that, if care is taken to avoid the reaction of O_2 with NO to form NO_2, the complexes [$Rh_2(\mu$-$O_2CR)_4(NO)_2$] (R = Me, Et, Pr) can be isolated in pure form. Here, we provide a more complete description of the reactivity of dirhodium tetracarboxylate complexes with NO. We also report that NO can reversibly displace a bound fluorophore axial ligand in solution with concomitant light emission upon excitation at the proper wavelength. The observed reversible fluorescence response of these dirhodium-fluorophore conjugates may ultimately allow their use for imaging biological NO.

Experimental Section

General Considerations. All reagents including [$Rh_2(\mu$-$O_2CMe)_4$] (**1**) were purchased from Aldrich or Alfa Aesar and used without further purification. Dansyl-piperazine (**4**) was prepared according to a literature procedure.[25] The rhodium complexes, [$Rh_2(\mu$-$O_2CEt)_4$] (**2**)[26] and [$Rh_2(\mu$-$O_2CPr)_4$] (**3**),[27] were synthesized according to published procedures. Methylene chloride (CH_2Cl_2) was purified by passage through alumina columns under an Ar atmosphere.[28] 1,2-Dichloroethane (DCE) was purified by distillation under an N_2 atmosphere over calcium hydride. Other solvents were used as received. Nitric oxide (Matheson 99%) was purified by a method adapted from the literature.[29] The NO stream was passed through an Ascarite (NaOH fused on silica gel) column and a 6 ft coil filled with silica gel cooled to −78 °C. For fluorescence experiments, NO was transferred to an anaerobic fluorescence cuvette with a gastight syringe. To eliminate the possibility of O_2 contamination, the syringe transfer was performed in an MBraun inert atmosphere glovebox. Fluorescence emission spectra were recorded at 25.0 ± 0.2 °C on a Hitachi F-3010 or Photon Technology International fluorescence spectrophotometer. NMR spectra were recorded on a Bruker DPX-400 spectrometer at ambient temperature and referenced to internal ^1H and ^{13}C solvent peaks.

Dansyl-imidazole (5). To a solution of dansyl chloride (500 mg, 1.85 mmol) in 5 mL of THF were added imidazole (126 mg, 1.85 mmol) and Cs_2CO_3 (1.3 g, 4.0 mmol). The reaction was allowed to stir overnight, filtered, and the solvent was removed by rotary evaporation. Crystallization of the crude product from hot EtOAc and hexanes gave yellow-green needles of **5** (520 mg, 93%): mp 100−101 °C. ^1H NMR (400 MHz, CD_2Cl_2): δ 8.67 (1H, d, J = 9.5 Hz), 8.38 (1H, dd, J = 7.5, 1.2 Hz), 8.26 (1H, d, J = 8.6 Hz), 8.10 (1H, s), 7.63−7.59 (2H, m), 7.32 (1H, t, J = 1.4 Hz), 7.21 (1H, d, J = 7.2 Hz), 7.01 (1H, s), 2.86 (6H, s). ^{13}C NMR (100 MHz, CD_2Cl_2): δ 153.0, 137.3, 133.8, 133.3, 131.3, 131.1, 130.4, 130.1, 129.9, 123.8, 118.4, 117.6, 116.3, 45.7.

[$Rh_2(\mu$-$O_2CMe)_4$(Ds-im)$_2$] (6). To a solution of [$Rh_2(\mu$-$O_2CMe)_4$] (50 mg, 0.11 mmol) in 5 mL of CH_3CN was added **5** (69 mg, 0.23 mmol). Over 30 min, a red-orange precipitate formed. X-ray quality crystals of [$Rh_2(\mu$-$O_2CMe)_4$(Ds-im)$_2$] (79 mg, 69%) were prepared by recrystallization of the crude solid by vapor diffusion (Et_2O/$CHCl_3$). ^1H NMR (400 MHz, CD_2Cl_2): δ 8.84 (2H, t, J = 1.1 Hz), 8.74 (2H, dd, J = 8.5, 0.9 Hz), 8.59 (2H, dd, J = 7.5, 1.2 Hz), 8.48 (2H, d, J = 8.7 Hz), 7.73 (4H, d, J = 1.1 Hz), 7.70−7.66 (4H, m), 7.25 (2H, d, J = 7.4 Hz), 2.89 (12H, s), 1.78 (12H, s). ^{13}C NMR (100 MHz, CD_2Cl_2): δ 191.8, 153.3, 138.6, 134.3, 132.7, 131.9, 131.1, 130.7, 130.3, 130.1, 123.9, 119.3, 117.6, 116.5, 45.7, 23.9. IR (KBr, cm^{-1}): 3135, 2940, 2835, 2791, 1595, 1528, 1457, 1430, 1410, 1367, 1343, 1311, 1233, 1202, 1174, 1157, 1101, 1052, 942, 919, 787, 736, 694, 679, 635, 594, 559, 536, 491. Anal. Calcd for $C_{38}H_{42}N_6O_{12}S_2Rh_2$: C, 43.69; H, 4.05; N, 8.04. Found: C, 43.58; H, 3.85; N, 8.01.

[$Rh_2(\mu$-$O_2CMe)_4$(Ds-pip)$_2$]·$CHCl_3$ (7·$CHCl_3$). To a solution of [$Rh_2(\mu$-$O_2CMe)_4$] (50 mg, 0.11 mmol) in 3 mL of CH_3CN was added **4** (70 mg, 0.22 mmol) in 1 mL of CH_3CN. The dark burgundy solution was allowed to stir for 4 h, and the solvent was removed by rotary evaporation. Burgundy crystals of **7**·$CHCl_3$ (102 mg, 77%) were grown by vapor diffusion (Et_2O/$CHCl_3$). Solvent-free X-ray quality crystals were prepared by vapor diffusion (pentane/toluene). ^1H NMR (400 MHz, CD_2Cl_2): δ 8.56 (2H, d, J = 8.5 Hz), 8.45 (2H, d, J = 8.7 Hz), 8.22 (2H, dd, J = 7.3, 1.2 Hz), 7.58−7.52 (4H, m), 7.19 (2H, d, J = 8.2 Hz), 3.57 (16H, bs), 2.86 (12H, s), 1.52 (12H, s). ^{13}C NMR (100 MHz, CD_2Cl_2): δ 190.8, 152.3, 134.0, 131.1, 131.0, 130.9, 130.6, 128.4, 123.7, 120.2, 115.7, 47.8, 45.9, 45.7, 23.6. IR (KBr, cm^{-1}): 3294, 3025, 2982, 2924, 2865, 1662, 1593, 1490, 1446, 1406, 1358, 1346, 1307, 1246, 1204, 1185, 1158, 1127, 1096, 1080, 1050, 965, 941, 883, 833, 801, 776, 752, 696, 666, 651, 621, 564, 541, 532, 498, 478, 444. Anal. Calcd for $C_{41}H_{55}Cl_3N_6O_{12}S_2Rh_2$: C, 41.03; H, 4.62; N, 7.00. Found: C, 41.14; H, 4.32; N, 6.62.

[$Rh_2(\mu$-$O_2CMe)_4(NO)_2$] (8). To a septum-capped vial containing a slurry of [$Rh_2(\mu$-$O_2CMe)_4$] (50 mg, 0.11 mmol) in 2 mL of chlorobenzene under a N_2 atmosphere was added NO (8.2 mL, 0.34 mmol) by means of a gastight syringe. Upon addition of NO, the solution turned dark burgundy and the solid [$Rh_2(\mu$-$O_2CMe)_4$] slowly dissolved. After being stirred for 2 h, the burgundy solution was filtered quickly through Celite and recrystallized by vapor diffusion (chlorobenzene/pentane) under a N_2 atmosphere containing 2 equiv of NO. After 1 week, dark burgundy blocks of **8** (28.2 mg, 49%) suitable for X-ray analysis were harvested. IR (KBr, cm^{-1}): 3418, 1729, 1694, 1580, 1427, 1348, 1047, 696, 628. Anal. Calcd for $C_8H_{12}N_2O_{10}Rh_2$: C, 19.14; H, 2.41; N, 5.58. Found: C, 19.02; H, 2.23; N, 5.71.

[$Rh_2(\mu$-$O_2CEt)_4(NO)_2$] (9). To a septum-capped vial containing a suspension of [$Rh_2(\mu$-$O_2CEt)_4$] (50 mg, 0.10 mmol) in 10 mL of pentane under an N_2 atmosphere was added NO (8.0 mL, 0.30 mmol) by means of a gastight syringe. On stirring, the solid green [$Rh_2(\mu$-$O_2CEt)_4$] complex slowly dissolved as the solution turned dark burgundy. After being stirred overnight, the burgundy solution was filtered through Celite, concentrated to a volume of 5 mL in vacuo, and placed in a sealed vial under a N_2 atmosphere containing 2 equiv of NO. X-ray quality burgundy blocks of **9** (42 mg, 75%) were prepared by crystallization from the pentane solution at −40 °C. IR (KBr, cm^{-1}):

(20) Varnes, A. W.; Dodson, R. B.; Wehry, E. L. *J. Am. Chem. Soc.* **1972**, *94*, 946−950.
(21) Franz, K. J.; Singh, N.; Spingler, B.; Lippard, S. J. *Inorg. Chem.* **2000**, *39*, 4081−4092.
(22) Boyar, E. B.; Robinson, S. D. *Coord. Chem. Rev.* **1983**, *50*, 109−208.
(23) Johnson, S. A.; Hunt, H. R.; Neumann, H. M. *Inorg. Chem.* **1963**, *2*, 960−962.
(24) Koh, Y.-B. Metal−Metal Bonding in Dirhodium Tetracarboxylates Trans Influence and Dependence of the Rhodium−Rhodium Bond Distance Upon the Nature of Axial Ligands. Ph.D. Thesis, The Ohio State University, Columbus, OH, 1979.
(25) Saavedra, J. E.; Booth, M. N.; Hrabie, J. A.; Davies, K. M.; Keefer, L. K. *J. Org. Chem.* **1999**, *64*, 5124−5131.
(26) Kitchens, J.; Bear, J. L. *Thermochim. Acta* **1970**, *1*, 537−544.
(27) Drago, R. S.; Long, J. R.; Cosmano, R. *Inorg. Chem.* **1981**, *20*, 2920−2927.
(28) Pangborn, A. B.; Giardello, M. A.; Grubbs, R. H.; Rosen, R. K.; Timmers, F. J. *Organometallics* **1996**, *15*, 1518−1520.
(29) Lorković, I. M.; Ford, P. C. *Inorg. Chem* **2000**, *39*, 632−633.

3393, 2984, 2943, 2881, 1698, 1672, 1581, 1464, 1418, 1375, 1300, 1076, 1012, 886, 810, 705, 650. Anal. Calcd for $C_{12}H_{20}N_2O_{10}Rh_2$: C, 25.83; H, 3.61; N, 5.02. Found: C, 26.02; H, 3.63; N, 5.04.

[Rh$_2$(μ-O$_2$CPr)$_4$(NO)$_2$] (10). To a septum-capped vial containing a suspension of [Rh$_2$(μ-O$_2$CPr)$_4$] (50 mg, 0.09 mmol) in 3 mL of pentane under a N_2 atmosphere was added NO (5.4 mL, 0.23 mmol) using a gastight syringe. On stirring, the green solid slowly dissolved as the solution turned dark burgundy. After being stirred overnight, the burgundy solution was filtered through Celite, concentrated to a volume of 1.5 mL in vacuo, and placed in a sealed vial under a N_2 atmosphere containing 2 equiv of NO. X-ray quality burgundy blocks of **10** (33.6 mg, 61%) were prepared by crystallization from the pentane solution at −40 °C. IR (KBr, cm^{-1}): 3405, 2961, 2930, 2874, 1687, 1579, 1412, 1348, 1314, 1266, 1101, 799, 735, 667. Anal. Calcd for $C_{16}H_{28}N_2O_{10}Rh_2$: C, 31.29; H, 4.59; N, 4.56. Found: C, 31.45; H, 4.57; N, 4.48.

Aqueous Solution Fluorescence Experiments. The experimental apparatus consisted of a 20 mL vessel containing a smaller 2 mL vial. The internal small vial was filled with a CH_2Cl_2 solution of [Rh$_2$(μ-O$_2$CMe)$_4$] (40 μM) and Ds-pip (20 μM). This vial was sealed with a screw cap fitted with 2−3 mm thick septum made from Silastic Q7-4656 biomedical grade ETR elastomer, an NO permeable polymer, which was purchased from Dow Corning. The external 20 mL vessel containing the 2.0 mL vial was capped and placed under a N_2 atmosphere, after which a saturated aqueous NO solution (15 mL) was transferred into it by a gastight syringe. An aqueous solution saturated with NO was prepared by bubbling a stream of NO gas into deionized water for 30 min at 25 °C. All procedures were performed under an anaerobic atmosphere. The fluorescence response was monitored by digital photography of the experimental apparatus with long-wavelength UV illumination from a hand-held UV lamp model UVGL-25 purchased from VWR International.

X-ray Crystallography. Single crystals suitable for data collection were covered in Infineum V8512 oil (formerly called Paratone N oil), mounted on the tips of quartz capillary tubes, and transferred to the −100 °C N_2 stream of a Bruker KRYOFLEX BVT-AXS nitrogen cryostat. Data were collected on a Bruker APEX CCD X-ray diffractometer (Mo Kα λ = 0.71073 Å) controlled by the SMART software package running on a Pentium III PC.[30] The general procedures used for data collection are reported elsewhere.[31] Empirical absorption corrections were calculated with the SADABS program.[32] Structures were solved and refined with the SHELXTL and SAINTPLUS software packages on a Pentium III PC running the Windows NT operating system.[33,34] All non-hydrogen atoms were refined anisotropically by least-squares cycles and Fourier syntheses. Hydrogen atoms were assigned idealized positions and given thermal parameters of 1.2 times the thermal parameter of the carbon or nitrogen atom to which each was attached. All structure solutions were checked for higher symmetry with the PLATON program.[35]

Results and Discussion

Synthesis of Fluorophore-Derivatized and Nitrosyl Dirhodium Complexes. Dirhodium tetraacetate complexes of dansyl-imidazole or dansyl-piperazine[25] were prepared by reaction of **1** with 2 equiv of the fluorophore in acetonitrile in 69% or 77% yield after crystallization, respectively (Scheme 1). Synthesis of the dinitrosyl complexes **8**, **9**, and **10** was accomplished by exposure of the appropriate dirhodium tetracarboxylate to 2.5 or 3 equiv of NO in chlorobenzene for **8** or in pentane for **9** and **10** (Scheme 2). Inadvertent leakage of dioxygen into the reaction vessels containing excess NO altered the characteristic burgundy color of the dinitrosyl complexes to brown, indicating formation of [Rh$_2$(μ-O$_2$CR)$_4$(NO)(NO$_2$)].[24] Crystallization of the dinitrosyl complexes required the presence of excess NO gas in the crystallization chambers to prevent NO loss and recovery of only free dirhodium tetracarboxylate. Complex **8** was isolated in 49% yield by allowing pentane vapor to diffuse into a burgundy-colored chlorobenzene solution of the crude product. Dinitrosyl complexes **9** and **10** were isolated in up to 75% yields by crystallization from saturated pentane solutions cooled to −40 °C. In contrast to the synthesis of nitrosyl complexes **8**, **9**, and **10**, it was not possible to prepare the analogous dinitrosyl complex of [Rh$_2$(μ-O$_2$CCF$_3$)$_4$]. Attempts to isolate 1:1 complexes of [Rh$_2$(μ-O$_2$CR)$_4$] with the dansyl-containing ligands or NO were unsuccessful. This result is consistent with literature data. Of the approximately 200 dirhodium tetracarboxylate structures in the Cambridge Structural Database,[36] only three complexes are reported that contain a monodentate ligand bound in a 1:1 stoichiometry.

Scheme 1

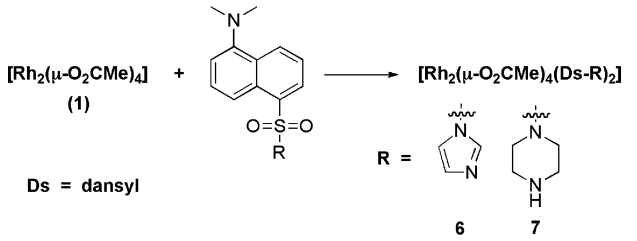

Scheme 2

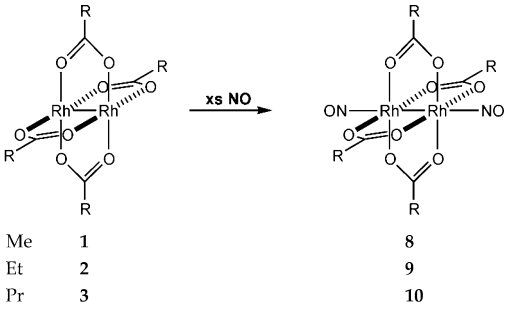

Structural Studies. The molecular structures of **6** and **7** are shown in Figure 1. Single-crystal X-ray diffraction results are given in Table S1, and selected bond distances and angles are presented in Table S2 (Supporting Information). The X-ray studies revealed fluorophore coordination at the axial sites of the dirhodium cores in **6** and **7** through the imidazole and piperazine N-atoms, respectively. The Rh−ligand and Rh−Rh distances in both structures are unremarkable and consistent with those of similar complexes reported in the literature (Table S2).[37]

Complexes **8**, **9**, and **10** are the first structurally characterized dinitrosyl adducts of any dirhodium tetracarboxylate and are depicted in Figures 2 and S1. A summary of the X-ray diffraction results indicating selected bond lengths and angles may be found in Tables S3 and S4 (Supporting Information).

(30) *SMART: Software for the CCD Detector System*, version 5.626; Bruker AXS: Madison, WI, 2000.
(31) Kuzelka, J.; Mukhopadhyay, S.; Spingler, B.; Lippard, S. J. *Inorg. Chem.* **2004**, *43*, 1751−1761.
(32) Sheldrick, G. M. *SADABS: Area-Detector Absorption Correction*; University of Göttingen: Göttingen, Germany, 2001.
(33) *SHELXTL: Program Library for Structure Solution and Molecular Graphics*, version 6.2; Bruker AXS: Madison, WI, 2001.
(34) *SAINTPLUS: Software for the CCD Detector System*, version 5.01; Bruker AXS: Madison, WI, 1998.
(35) Spek, A. L. *PLATON, A Multipurpose Crystallographic Tool*; Utrecht University: Utrecht, The Netherlands, 2000.
(36) Allen, F. H. *Acta Crystallogr., Sect. B* **2002**, *B58*, 380−388.
(37) Cotton, F. A.; Walton, R. A. *Multiple Bonds Between Metal Atoms*, 2nd ed.; Oxford University Press: Oxford, England, 1993.

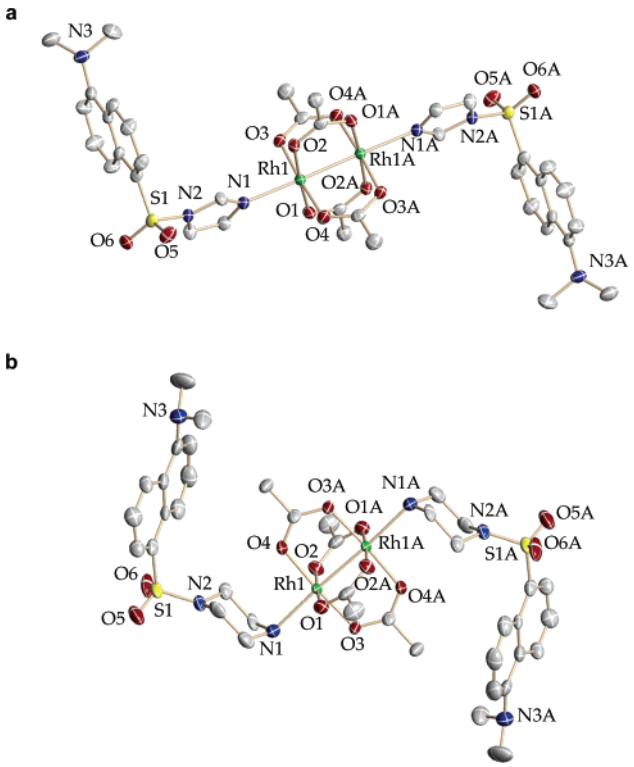

Figure 1. ORTEP diagrams showing 50% probability thermal ellipsoids and selected atom labels for (a) $[Rh_2(\mu\text{-}O_2CMe)_4(Ds\text{-}im)_2]$ (**6**) and (b) $[Rh_2(\mu\text{-}O_2CMe)_4(Ds\text{-}pip)_2]$ (**7**).

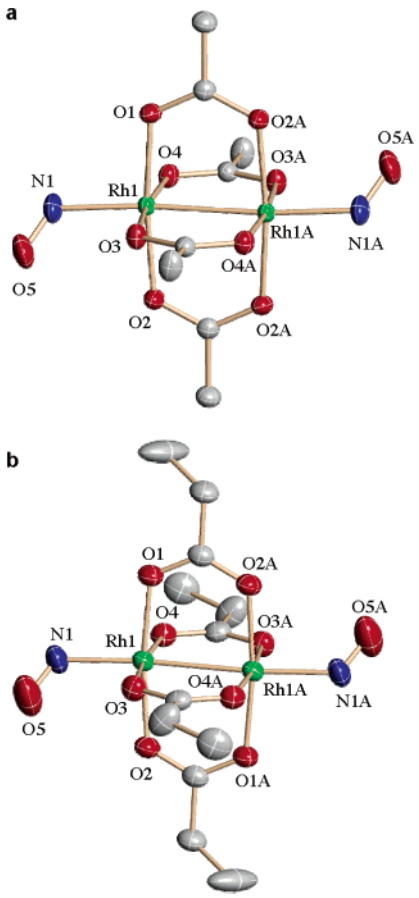

Figure 2. ORTEP diagrams showing 50% probability thermal ellipsoids and selected atom labels for (a) $[Rh_2(\mu\text{-}O_2CMe)_4(NO)_2]$ (**8**) and (b) $[Rh_2(\mu\text{-}O_2CEt)_4(NO)_2]$ (**9**).

Structurally, all three dinitrosyl species are very similar. The observed Rh−N axial ligand distances of 1.945(3)−1.958(3) Å are some of the shortest known for dirhodium tetracarboxylate complexes.[37] The only complex having a shorter Rh−axial ligand bond length is the related $[Rh_2(\mu\text{-}O_2CMe)_4(NO)(NO_2)]$ compound, in which the Rh−NO bond is 1.927(4) Å.[24] The Rh−Rh bond distances for the three dinitrosyl complexes are also quite remarkable. These distances, 2.512(1) and 2.5191(9) Å for **9** and **10**, are the longest yet observed for dirhodium tetracarboxylate complexes having N-donor axial ligands. The lengthening of the Rh−Rh bond is consistent with a previous analysis of metal−metal bonding in dirhodium tetracarboxylate complexes, which is discussed in detail elsewhere.[38] Again, the only similar reported Rh−Rh distance is the 2.4537(4) Å value in $[Rh_2(\mu\text{-}O_2CMe)_4(NO)(NO_2)]$.[24] The N−O bond lengths in **8**, **9**, and **10**, which fall between 1.131(4) and 1.150(3) Å, are also quite similar. Although still small, the largest geometric variation among the complexes occurs in the Rh−N−O bond angles. One of the two crystallographically independent molecules of **10** has an angle of 122.7(3)°, which is 1.9° larger than the corresponding value from **9**. As with $[Rh_2(\mu\text{-}O_2CMe)_4(NO)(NO_2)]$, the bent nitrosyl ligands in **8**, **9**, and **10** are positioned between the two planes defined by the bridging carboxylate ligands to minimize intramolecular nonbonding contacts with their oxygen atoms.

The dinitrosyl complexes can be viewed as two separate octahedral $\{MNO\}^8$ units in the standard notation, where the superscript represents the sum of metal d electrons and the unpaired π^* electron from the nitrosyl.[39] The nearly idealized bent geometries of the nitrosyl ligands in the three complexes, the average Rh−N−O angle being 121.4°, are consistent with the structure expected of an octahedral $\{MNO\}^8$ complex, which results from population of the antibonding molecular orbital formed by the metal d_{xy} and d_{yz} orbitals and the NO π^* orbital. The related $[Ru_2(\mu\text{-}O_2CEt)_4(NO)_2]$ complex, which can be viewed as two adjacent $\{MNO\}^7$ centers, overall has two fewer d electrons than the dirhodium dinitrosyls, and an Ru−N−O angle of 152.4° that is intermediate between the idealized bent and linear geometries.[40] If an analogous group 7 transition-metal tetracarboxylate complex were to exist, it would consist of two $\{MNO\}^6$ metal centers. As with other $\{MNO\}^6$ complexes, one would predict it to have linear nitrosyl ligands because of the lack of electrons to populate the antibonding molecular orbital formed by the metal d_{xy} and d_{yz} orbitals and the NO π^* orbital.

Chemical Reactivity Studies. The interactions of the dirhodium complexes **1**, **2**, and **3** with the dansyl-containing ligands **4** and **5** are similar to those observed for other ligands that coordinate to the axial sites of the dirhodium tetraacetate core.[22] In solution, both 1:1 and 1:2 adducts with these bases are apparent, as revealed by absorption spectral titrations that exhibit clear isosbestic points for the equilibria given by eqs 1 and 2, respectively (Figure 3).

$$[Rh_2(\mu\text{-}O_2CR)_4] + L \rightleftharpoons [Rh_2(\mu\text{-}O_2CR)_4(L)] \quad (1)$$

$$[Rh_2(\mu\text{-}O_2CR)_4(L)] + L \rightleftharpoons [Rh_2(\mu\text{-}O_2CR)_4(L)_2] \quad (2)$$

The reactions of **1**, **2**, and **3** with NO are extremely fast. Preliminary stopped-flow studies of the reaction of **3** with excess

(38) Christoph, G. G.; Koh, Y.-B. *J. Am. Chem. Soc.* **1979**, *101*, 1422−1434.
(39) Enemark, J. H.; Feltham, R. D. *Coord. Chem. Rev.* **1974**, *13*, 339−406.

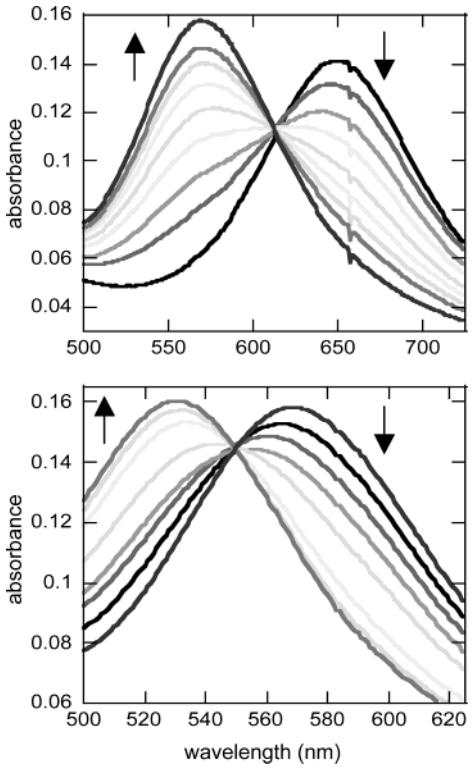

Figure 3. Absorption spectra for the titration of 50 μM [$Rh_2(\mu$-$O_2CMe)_4$] (**1**) with dansyl-piperazine (**4**) in DCE at 25.0 ± 0.1 °C. Addition of **4** to **1**, as shown in the top panel, decreases the initial absorbance maximum at 648 nm, and a new feature grows in at 568 nm, indicating formation of the 1:1 adduct. Traces correspond to final concentrations of 0, 5, 10, 15, 20, 25, 30, 35, and 45 μM quantities of **4**. In the bottom panel, as additional aliquots of **4** are administered, the 568 nm absorption band is replaced by a third feature at 530 nm, which indicates formation of [$Rh_2(\mu$-$O_2CMe)_4$-(Ds-pip)$_2$] (**7**). Starting with the 568 nm absorbance maximum trace, the spectra correspond to final concentrations of 50, 60, 70, 80, 90, 100, 150, 200, and 250 μM **4**.

NO showed complete formation of the dinitrosyl species within the 1-ms mixing time of the instrument at −80 °C. This result corresponds to an approximate on-rate of at least 4×10^6 s^{-1} at 40 °C. Such a value indicates the potential of the dirhodium tetracarboxylate scaffold for real-time imaging of NO changes in biological fluids.

By analogy to previously characterized systems, NO should sequentially form mono- and dinitrosyl complexes with dirhodium tetracarboxylates. We were unable, however, to distinguish the mono- and dinitrosyl adducts by IR spectroscopy in solution. Titration experiments revealed the formation of a single nitrosyl band at 1698 cm^{-1} for the reaction of **3** with NO in DCE at room temperature (Figure 4). As with the fluorophore adducts of **1**, it was not possible to isolate and characterize structurally the 1:1 complexes of NO with **1**, **2**, and **3**.

All three dinitrosyl complexes display similar ν_{NO} bands in the solid state. IR spectra of single crystals of **8** and **9** each show one broad and one sharp ν_{NO} band, respectively, at 1729 and 1694 cm^{-1} for **8** and 1698 and 1672 cm^{-1} for **9**. In solution, the 1729 and 1694 cm^{-1} bands from **8** convert to a single nitrosyl band at 1702 cm^{-1}. Similar behavior was previously observed with [$Ru_2(\mu$-$O_2CEt)_4(NO)_2$].[40] In the case of **10**, only a single broad ν_{NO} band at 1687 cm^{-1} is observed in the solid

(40) Lindsay, A. J.; Wilkinson, G.; Motevalli, M.; Hursthouse, M. B. *J. Chem. Soc., Dalton Trans.* **1987**, 2723−2736.

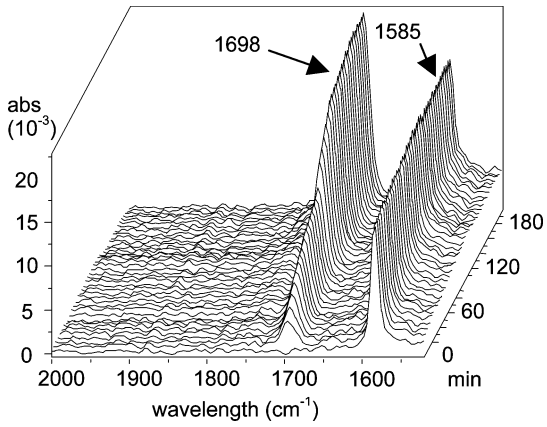

Figure 4. Solution IR spectra of the reaction of [$Rh_2(\mu$-$O_2CPr)_4$] with NO in DCE at room temperature. The first aliquot of 1 equiv of NO was added at $t = 0$ min, and a second equiv was added at $t = 60$ min.

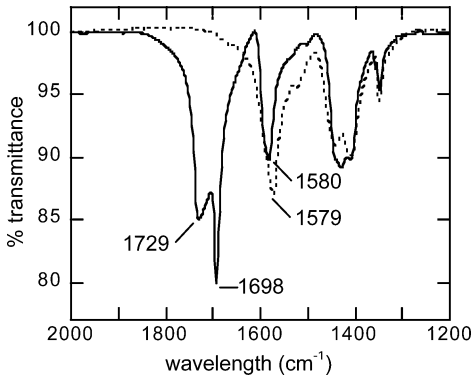

Figure 5. IR spectra (KBr) of [$Rh_2(\mu$-$O_2CMe)_4(NO)_2$] (**8**), solid line, and [$Rh_2(\mu$-$O_2CMe)_4$] (**1**), dashed line, formed by allowing a DCE solution of **8** to stand in air.

state, which shifts to 1698 cm^{-1} in DCE solution. Figure 5 shows an overlay of the solid IR spectra of **1** and **8**, the only significant difference between the two being the presence of the nitrosyl stretching bands in **8**. The absence of a large shift in the carboxylate C−O stretching band upon formation of the dinitrosyl adduct indicates that the dirhodium core remains intact and undergoes very little change.

Like the parent dirhodium complexes, **8**, **9**, and **10** are air-stable, and their spectroscopic properties revealed no evidence for decomposition of the dirhodium core. Although the core is stable, in solution the dinitrosyl complexes lose NO and reform the corresponding parent complex. At room temperature, solids **8**, **9**, and **10** also slowly lose NO over a period of several days, but the adducts are stable for several months when stored at −80 °C. The observed NO chemistry of these dirhodium compounds opens the possibility for their application as reversible NO sensors in biological systems.

Fluorescence Spectroscopic Studies. Solutions of **6** and **7** in DCE emit only weakly when excited at 365 nm for Ds-im or at 345 nm for Ds-pip. Neither complex is fluorescent in the solid state. Titrations with [$Rh_2(\mu$-$O_2CMe)_4$] indicate maximal fluorescence quenching upon addition of 4 and 2 equiv of [$Rh_2(\mu$-$O_2CMe)_4$] with Ds-im and Ds-pip, respectively. Based on the previous absorption spectroscopy titrations, vide supra, these ligand-to-[$Rh_2(\mu$-$O_2CMe)_4$] ratios correspond to formation of the 1:1 adducts.

Exposure of a solution of 10 μM Ds-im and 40 μM [$Rh_2(\mu$-$O_2CMe)_4$] in DCE to 100 equiv of NO results in an immediate

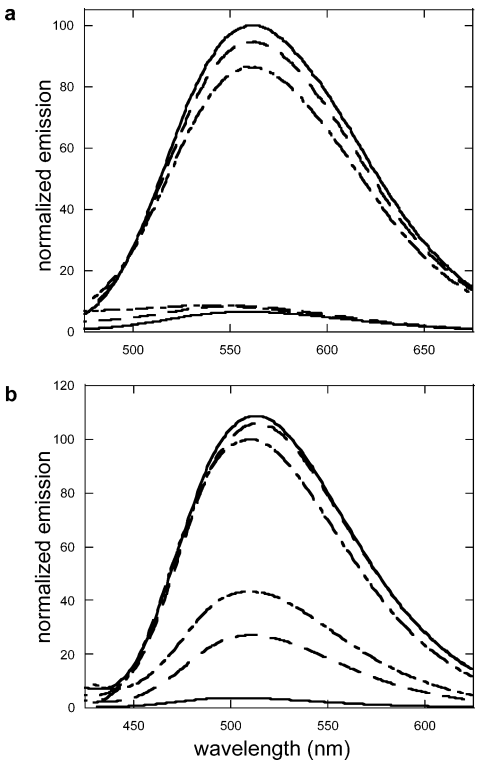

Figure 6. Fluorescence emission spectra showing the reversible fluorescence response of 10 μM Ds-im and 40 μM [$Rh_2(\mu$-$OAc)_4$] (a) and 10 μM Ds-pip with 20 μM [$Rh_2(\mu$-$OAc)_4$] (b) in DCE. The upper set of solid, dashed, and dashed−dot lines are after the first, second, and third additions of 100 equiv of NO, respectively. The lower set of corresponding lines are before admission of NO and after the first and second 30 min Ar purges. Excitation is at 365 nm for the Ds-im system and at 350 nm for the Ds-pip system.

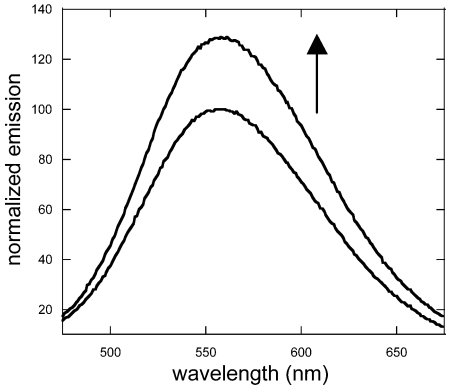

Figure 7. Fluorescence spectra of 10 μM Ds-im (**4**) and 40 μM [$Rh_2(\mu$-$O_2Me)_4$] (**1**) in DCE after exposure to 1 equiv of NO showing a 27% increase in integrated fluorescence emission.

16-fold increase in the integrated fluorescence intensity. A similar 26-fold increase in integrated fluorescence intensity is observed after introduction of 100 equiv of NO to a DCE solution containing 10 μM Ds-pip and 20 μM [$Rh_2(\mu$-$O_2CMe)_4$]. In both systems, the fluorescence response is reversible. A 30 min Ar purge to remove the excess NO restores the fluorescence, and this cycle can be repeated at least three times (Figure 6).

The reaction of 1 equiv of NO with the [$Rh_2(\mu$-$O_2CMe)_4$-(Ds-im)] complex gives a 27% increase in integrated fluorescence (Figure 7). Thus, only 1 equiv of the neurotransmitter is necessary to displace the coordinated fluorophore (Scheme 3),

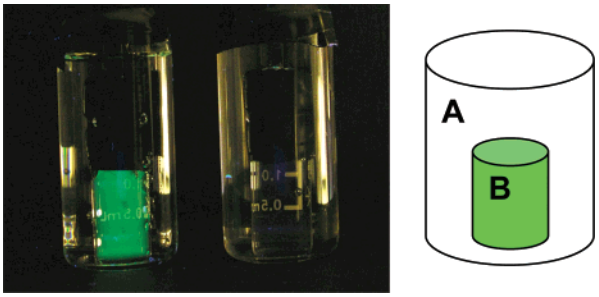

Figure 8. Left: a photo monitoring the fluorescence response in the reaction of [$Rh_2(\mu$-$O_2CMe)_4$(Ds-pip)] and NO. Vials from left to right: saturated aqueous NO solution and aqueous control. Right: experimental apparatus with the Silastic membrane separating vials A and B. Vial A contains a 15 mL aqueous solution saturated with NO, and vial B contains 1.5 mL of a CH_2Cl_2 solution of 40 μM [$Rh_2(\mu$-$O_2CMe)_4$] and 20 μM Ds-pip.

Scheme 3

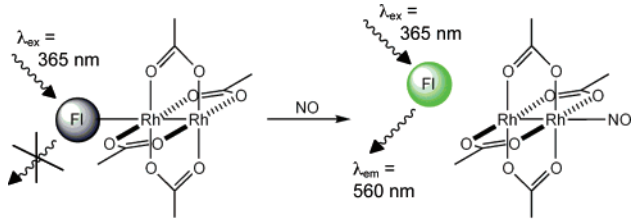

although we do not know at present whether this reaction occurs by an associative or dissociative mechanism.

To determine the sensitivity of the Ds-im complex for nitric oxide, sequentially decreasing volumes of NO gas were added to aliquots of 2 μM Ds-im and 4 μM [$Rh_2(\mu$-$O_2CMe)_4$] in DCE. From this experiment, we estimate a detection limit of 4−8 μM NO. Greater sensitivity should be possible in the absence of excess, nonfluorophore-bound [$Rh_2(\mu$-$O_2CMe)_4$].

Although dirhodium tetraacetate is water-soluble and air-stable, the current fluorophore adducts do not function as NO sensors in an aqueous environment. Water may compete with the fluorophore for coordination to the dirhodium core. One strategy to achieve aqueous solution compatibility is to isolate the sensor solution behind a NO-permeable membrane that is impervious to water. A Silastic polymer-based membrane was chosen to test this possibility. Silastic tubing has demonstrable NO permeability and has previously been used for admission of NO to aqueous solutions.[41] The fluorescence response of a 40 μM [$Rh_2(\mu$-$O_2CMe)_4$] and 20 μM Ds-pip solution in CH_2Cl_2, sequestered from a saturated aqueous NO solution by the Silastic membrane, and the experimental setup are shown in Figure 8. Fluorescence emission was observed immediately after admission of the NO-containing aqueous solution into the outer vial. Titration experiments with sequentially decreasing amounts of NO demonstrated a fluorescence response visible by the naked eye at NO concentrations as low as 100 μM. In addition, the Silastic membrane is well suited for isolating the dirhodium tetracarboxylate fluorophore conjugates from reactions with other, nongaseous Lewis bases that might displace the fluorophore and give a false reading. When an aqueous solution containing 50 mM pyridine was introduced into the outer vial, no fluorescence response occurred (Figure S2). These experiments thus illustrate a potential approach for imaging biological NO based upon dirhodium tetracarboxylate coordination chemistry.

(41) Wang, C.; Deen, W. M. *Ann. Biomed. Eng.* **2003**, *31*, 65−79.

Conclusions

Dirhodium tetracarboxylate complexes containing bound fluorophore conjugates react directly, rapidly, and reversibly with NO. The resulting dinitrosyl adducts have been completely characterized, losing NO upon standing in air. The reactivity of the fluorophore conjugated dirhodium complexes with NO is fast, with on-rates indicating nearly instantaneous binding of the gas at 40 °C. Fluorescence detection methodologies based on the dirhodium platform hold promise for development into viable sensors for NO in biological systems. One potential route for the preparation of NO sensors using this system is to sequester the nonpolar dirhodium fluorophore solution from the surrounding aqueous environment by use of a NO-permeable polymer. Initial experiments demonstrate the potential utility of this strategy for the detection of aqueous NO.

Acknowledgment. This work was supported by NSF grant CHE-0234951. We thank Dr. Sumitra Mukhopadhyay for assistance with the X-ray structure determinations. The MIT DCIF NMR spectrometer was funded through NSF grant CHE-9808061.

Supporting Information Available: Tables S1−S4 reporting crystallographic data and interatomic distances and angles; Figures S1 and S2 illustrating the structure of **10** and the fluorescence control experiment with aqueous pyridine added to the outer vial (see text) (PDF); and X-ray crystallographic files (CIF). This material is available free of charge via the Internet at http://pubs.acs.org.

JA038471J